

# Turbulence Measurements in a Compressible Boundary Layer

WILLIAM C. ROSE\*

NASA Ames Research Center, Moffett Field, Calif.

The rms intensities of fluctuating mass flux and total temperature and their correlation coefficients are given for the case of an adiabatic, Mach 4, axisymmetric shock-wave boundary-layer interaction. Data were obtained upstream, within, and downstream of the interaction by the use of constant temperature hot-wire anemometer. Turbulence spectra are shown at selected locations. The measurements indicate that certain frequencies of the turbulence are increased as a result of the interaction and that the mass flux and total temperature fluctuations remain highly correlated over most of the boundary layer throughout the interaction. The present data are also transformed to rms intensities of fluctuating static temperature and velocity and compared with existing data obtained in adiabatic flows.

## Nomenclature

$a_w$	= overheating parameter, $(R_w - R_r)/R_r$
$E$	= bridge voltage
$f$	= frequency
$k$	= thermal conductivity
$M$	= Mach number
$Nu$	= Nusselt number
$p$	= pressure
$r$	= $-\Delta e_{pu}/\Delta e_T$
$R$	= resistance
$Re$	= Reynolds number
$R_{uT}$	= correlation coefficient for velocity and static temperature
$R_{(\rho u)T}$	= correlation coefficient for mass flux and total temperature
$T$	= temperature
$u$	= velocity component in streamwise direction
$x$	= streamwise coordinate, measured from cone tip
$y$	= cross-stream coordinate, measured from tunnel wall
$\delta$	= boundary-layer thickness
$\Delta e_{( )}$	= fluctuation sensitivity
$\eta$	= $T_r/T_i$
$\theta$	= $T_w/T_i$
$\tau_{wr}$	= $(T_w - T_r)/T_r$
$\mu$	= absolute viscosity

## Subscripts

$r$	= recovery conditions
$t$	= total conditions
$w$	= pertaining to wire
wall	= evaluated at the wall ( $y = 0$ )
$\delta$	= evaluated at $\delta$
$\infty$	= freestream conditions

## Superscripts

$( )'$	= fluctuating quantity
$( )$	= time-averaged quantity
$\langle ( ) \rangle$	= rms of fluctuating quantity

## Introduction

A PRIMARY goal of fluid mechanics research today is to develop computing techniques that can be used to predict the behavior of compressible, turbulent boundary-layer flows. If these techniques are to provide solutions for complex flows, they must incorporate realistic models of the turbulence. Nearly all of the present computing techniques for compressible flows rely heavily on empirical information obtained in incompressible flows.

Presented as Paper 73-167 at the AIAA 11th Aerospace Sciences Meeting, Washington, D.C., January 10-12, 1973; submitted January 26, 1973; revision received January 28, 1974.

Index categories: Boundary Layers and Convective Heat Transfer—Turbulent; Supersonic and Hypersonic Flow.

\* Research Scientist. Member AIAA.

Direct measurements of turbulence in compressible boundary layers have been made by relatively few investigators.<sup>1-9</sup> Of the investigations, only those of Grande<sup>6</sup> and Morkovin<sup>7</sup> deal with a flow that is different from a zero or near-zero pressure-gradient boundary layer. Morkovin's measurements were obtained in a strongly accelerated flow (favorable pressure gradient). Grande's measurements were obtained primarily in the flow external to the boundary layer in the vicinity of a shock-wave boundary-layer interaction (a strong adverse pressure gradient). Since almost all aerodynamic applications involve flows in adverse pressure gradients, there is a prime need for understanding the turbulence mechanics in these boundary-layer flows; particularly, the effect of pressure gradient on turbulence. Hence, there is a need for basic turbulence data taken in such flows.

The purpose of the present investigation was to obtain turbulence data within a boundary layer at several streamwise stations in a shock-wave induced adverse pressure gradient. The boundary layer upstream of the pressure gradient was one that developed on a nozzle wall and thus was not an equilibrium boundary layer. With the nonequilibrium nature of the upstream boundary layer in mind, the data presented here show the change brought about by an adverse pressure gradient in turbulence properties from their upstream state.

## Experimental Apparatus and Procedure

The experimental arrangement used in the present study is shown schematically in Fig. 1. The turbulent boundary layer used in this study was the one that developed on the wall of an axially symmetric nozzle and test section. The wall temperature

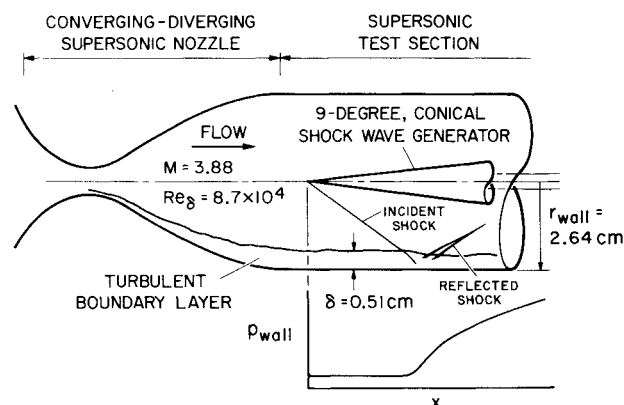


Fig. 1 Schematic of experimental arrangement.

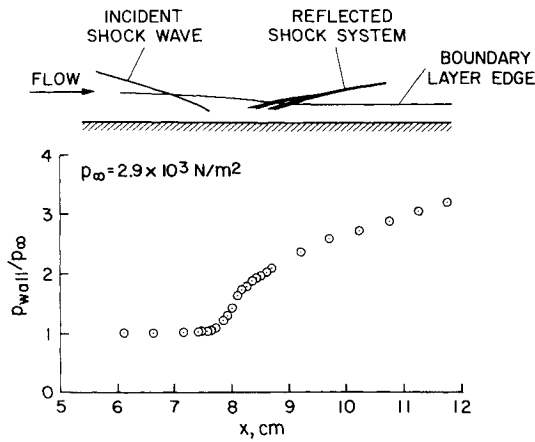


Fig. 2 Shock wave locations and surface-static pressure distribution.

was near the adiabatic wall temperature for the test section Mach number  $M = 3.88$ . The Reynolds number based on boundary-layer thickness was  $8.7 \times 10^4$ . The test section was 5.28 cm diam and the boundary-layer thickness was 0.51 cm. Total temperature and pressure were nominally 300°K and  $3.7 \times 10^5$  N/m<sup>2</sup>, respectively. The adverse pressure gradient was generated by a 9° half-angle cone placed on the centerline of the test section. The resulting incident-reflected shock wave configuration and surface pressure distribution are shown in Fig. 2. The flowfield sketch in Fig. 2 is to scale and is aligned with the pressure distribution. The pressure rise through the interaction was near that required for incipient separation of the boundary layer.

Distributions of the mean flow quantities at five streamwise stations upstream, within, and downstream of the interaction region are shown in Fig. 3. The wall velocity is zero while the remaining wall parameters are evaluated at the adiabatic wall temperature. Additional mean-flow data for this flow were given by Rose.<sup>10</sup>

The instrumentation used for obtaining the turbulence data consisted of the hot wire (sketched in Fig. 4) connected to a Disa 55D01 constant-temperature anemometer. The details of the

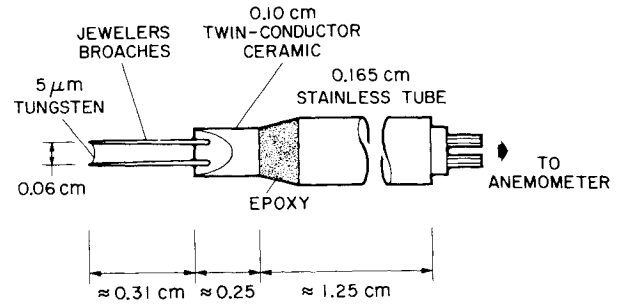


Fig. 4 Hot-wire probe.

operation of the anemometer unit to achieve a maximum bandwidth are discussed in Ref. 10. In that study it was shown, by the square-wave response test, that the upper frequency response was near 200 kHz. This response was adequate in the present study to resolve disturbances whose characteristic lengths were greater than about  $\delta/5$  in the outer part of the boundary layer and  $\delta/8$  in the lower part.

The fluctuating voltages from the hot-wire system were related to the fluctuations in physical flow variables by the Kovaszny<sup>11</sup> technique. The technique has been reviewed elsewhere<sup>1,10</sup> and is discussed below only in terms of the direct calibration used in the present study. For a wire held normal to the flow in a supersonic stream, a heated wire produces a fluctuating voltage response to fluctuating physical variables given by

$$E' = \Delta e_{T_t} \left( 100 \frac{T_t'}{T_t} \right) + \Delta e_{\rho u} \left( 100 \frac{(\rho u)'}{\bar{\rho} \bar{u}} \right) \quad (1)$$

The  $\Delta e_{( )}$  are the sensitivity coefficients for the respective physical variables. They have the form<sup>9</sup>

$$\Delta e_{\rho u} = \frac{\bar{E}}{200} \left[ \frac{\partial \ln Nu_t}{\partial \ln Re_t} - \frac{1}{\tau_{wr}} \frac{\partial \ln \eta}{\partial \ln Re_t} \right] \quad (2a)$$

$$\Delta e_{T_t} = \frac{\bar{E}}{200} \left[ n_t + 1 - \left\{ \frac{\partial \ln Nu_t}{\partial \ln \theta} + \frac{\theta}{\theta - \eta} \right\} \right] - m_t (\Delta e_{\rho u}) \quad (2b)$$

where

$$n_t = \frac{\partial \ln k_t}{\partial \ln T_t}$$

and

$$m_t = \frac{\partial \ln \mu_t}{\partial \ln T_t}$$

However, from Eq. (1) the sensitivities may be written directly as

$$\Delta e_{\rho u} = \frac{\bar{E}}{100} \frac{\partial \ln E}{\partial \ln \rho u} \quad (3)$$

$$\Delta e_{T_t} = \frac{\bar{E}}{100} \frac{\partial \ln E}{\partial \ln T_t}$$

The sensitivities in Eq. (3) were calibrated as follows: the value of  $\partial \ln E / \partial \ln \rho u$  was obtained from the slope of a logarithmic plot of  $E$  vs  $\rho u$  for the range of Reynolds and Mach numbers encountered in the boundary layer. The wire was mounted on the centerline of the tunnel and then driven to different locations in the nozzle to change Mach number. At each Mach number, the value of  $\rho u$  was changed while recording the voltage  $E$ .

The term  $(\partial \ln E / \partial \ln T_t)$  could not be determined accurately in the present study so Eq. (2b) was used with the following substitutions<sup>9</sup>

$$\left\{ \frac{\partial \ln Nu_t}{\partial \ln \theta} + \frac{\theta}{\theta - \eta} \right\} = 2K \left[ \frac{\partial \ln E}{\partial \ln R_w} + \left( \frac{1}{2} - \frac{R_w}{R_w + R_s} \right) \right]$$

where  $n_t = 0.885$  and  $m_t = 0.765$  and  $\Delta e_{\rho u}$  taken from the direct calibration discussed previously. The value of  $(\partial \ln E / \partial \ln R_w)$  is

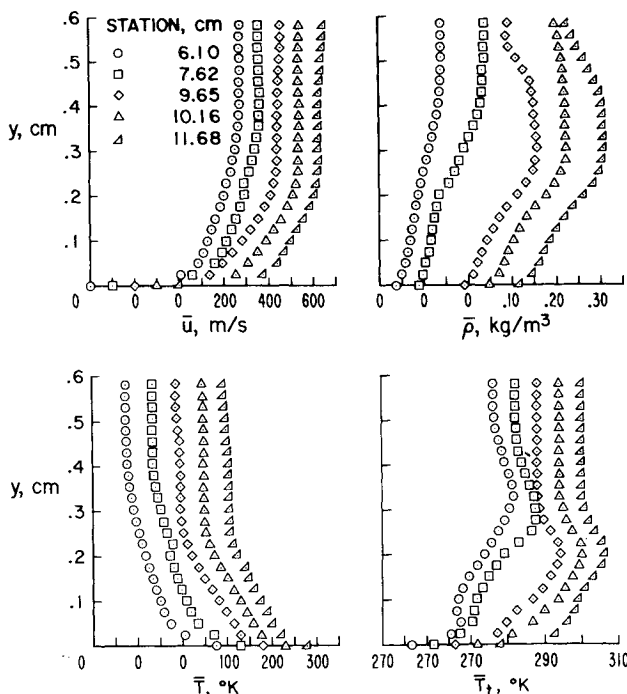


Fig. 3 Distribution of mean-flow properties through interaction.

obtained from a curve fit of the data taken at the time of the fluctuating measurements.

The resulting set of sensitivities therefore is obtained from terms that are either calibrated in place, calibrated beforehand, or are known physical properties of air and tungsten. These sensitivities are used to resolve the physical variables from the rms voltage fluctuations as follows:

$$\frac{\overline{E'^2}}{(\Delta e_{T_i})^2} = r^2 \frac{(\rho u)^2}{(\bar{\rho} \bar{u})^2} \cdot 10^4 - 2r \frac{(\rho u) T_i'}{\bar{\rho} \bar{u} \bar{T}_i} \cdot 10^4 + \frac{T_i'^2}{\bar{T}_i^2} \cdot 10^4 \quad (4)$$

where  $r = -\Delta e_{\rho u} / \Delta e_{T_i}$ .

The term  $(\rho u) T_i' / \bar{\rho} \bar{u} \bar{T}_i$  may be written as  $R_{(\rho u) T_i} [(\rho u)' / \bar{\rho} \bar{u}] \times (\bar{T}_i' / \bar{T}_i)$ . The ratio,  $r$ , changes with overheat ratio,  $a_w$ , so that

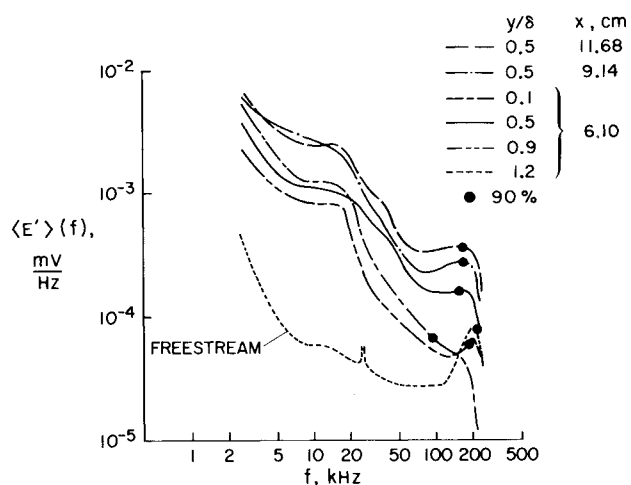


Fig. 6 Spectra of voltage fluctuations.

Eq. (4) may be solved for the physical variables and their correlation coefficient if data are obtained for at least three overheat ratios. In the present study, five overheat ratios were used. A least-squares technique was used to solve the resulting overdetermined linear system of simultaneous equations.

An indication of the spectral distribution of the turbulence was obtained by using a Krohn-Hite variable bandpass filter (Model 310-A). For these spectra measurements, the hot wire was operated at a single overheat ratio ( $a_w = 0.8$ ) so that the fluctuating voltages are primarily the result of mass-flux fluctuations. The spectra were obtained with a filter bandwidth of 5 kHz below 30 kHz and 10 kHz above 30 kHz.

In addition to the abovementioned information, oscilloscope traces of the hot-wire signal (again with  $a_w = 0.8$ ) were obtained at locations corresponding to those for which spectral data were obtained.

## Results

The results of the present investigation are shown graphically in Figs. 5 and 6. Figure 5a shows the rms fluctuations of mass flux,  $\langle(\rho u)'\rangle / \bar{\rho} \bar{u}$ , while Fig. 5b shows the total temperature  $\langle T_i' \rangle / \bar{T}_i$  and their correlation coefficient  $R_{(\rho u) T_i}$  at the same streamwise locations shown in Fig. 3. The distribution of  $\langle(\rho u)'\rangle / \bar{\rho} \bar{u}$  across the boundary layer at the upstream stations ( $x = 6.10$  and  $7.62$  cm) are significantly different than those downstream of the incident reflected shock system ( $x = 9.65$ ,  $10.16$ , and  $11.68$  cm). (See Fig. 2 for shock-wave locations.) The downstream boundary-layer thickness based on total temperature is approximately  $0.33$  cm compared with that upstream of  $0.51$  cm. This decrease in thickness across the interaction should be borne in mind when viewing Fig. 5. The fluctuations shown in Fig. 5a reflect this thickness change. In addition, the percentage fluctuation in the lower  $\frac{2}{3}$  of the boundary layer has risen from about  $16\%$  to about  $20\%$  on the average. Similar increases in fluctuation level are evident in the total temperatures shown in Fig. 5b. Again, in the lower part of the boundary layer the percentage total temperature fluctuations increase from an average of about  $0.8\%$  to about  $1.1\%$ .

The correlation coefficient remains between  $0.9$  and about  $1.0$  in the lower  $\frac{2}{3}$  of the layer and drops to negative values near the boundary-layer edge. Fluctuation diagrams<sup>11</sup> for the present data outside the boundary layer indicate that  $R_{(\rho u) T_i}$  is near the expected value of  $-1.0$ . The behavior of  $R_{(\rho u) T_i}$  for the present data show that mass flux and total temperature fluctuations are highly correlated in the lower  $\frac{2}{3}$  of the boundary layer upstream and remain so downstream of the interaction.

The velocity and static temperature fluctuations and their correlation coefficient at an upstream station and one downstream station are shown in Fig. 5c. These fluctuations were obtained by transforming<sup>9</sup> the measured  $\langle(\rho u)'\rangle / \bar{\rho} \bar{u}$ ,  $\langle T_i' \rangle / \bar{T}_i$ , and

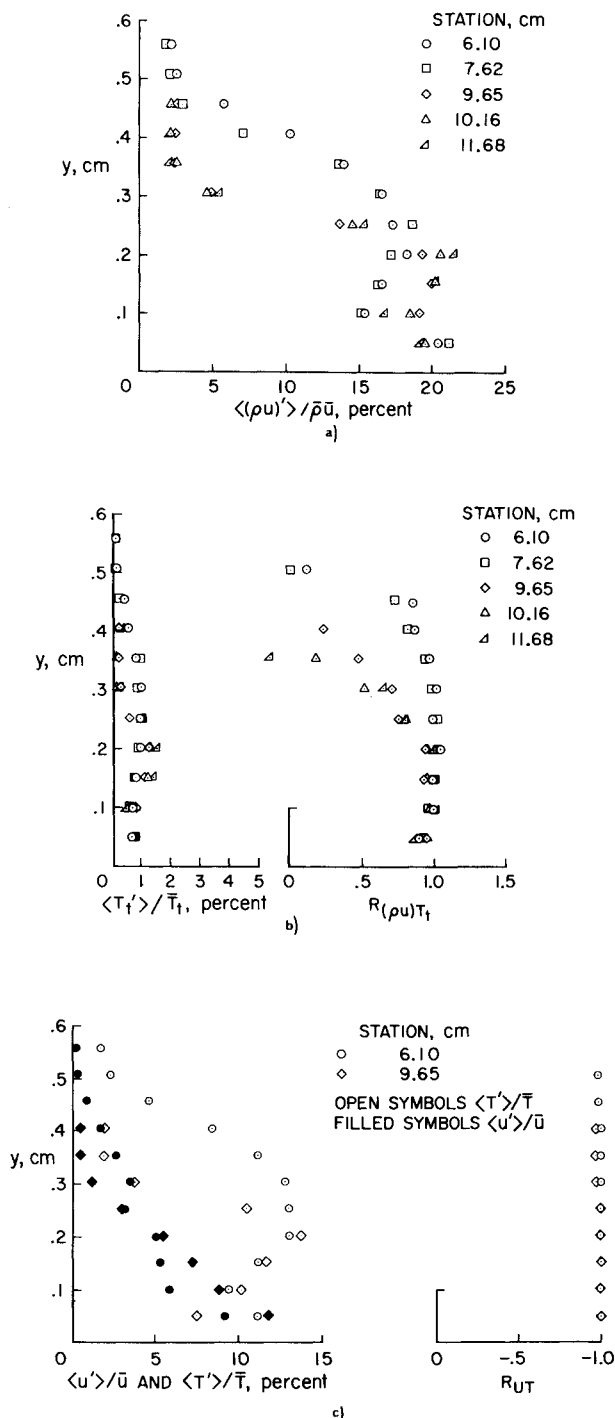


Fig. 5 Fluctuating-flow data. a) Mass flux fluctuations. b) Total temperature fluctuations and correlation coefficient. c) Velocity and static temperature fluctuations and correlation coefficient.

$R_{(\rho u)T}$  to  $\langle u' \rangle / \bar{u}$ ,  $\langle T' \rangle / \bar{T}$  and  $R_{uT}$ . The level of velocity fluctuations is increased at a given  $y/\delta$ , while that of the temperature fluctuations does not appear to be significantly increased as a result of the interaction. The correlation coefficient  $R_{uT}$  is essentially  $-1.0$  over the entire layer both upstream and downstream of the interaction. The behavior of  $R_{uT}$  (and of  $R_{(\rho u)T}$ ) support the concept<sup>5</sup> that the temperature fluctuations are produced by transport of the mean temperature field by velocity fluctuations.

The results of the spectra measurements are shown in Fig. 6. Also shown for each spectrum is the frequency below which 90% of the voltage occurs. The data were taken at the 6.10 cm station without the shock wave generator in the tunnel. Thus, the spectra at this station are free of any possible disturbances produced by the shock generator. Outside the boundary layer, at  $y/\delta = 1.2$  and below about 25 kHz, the spectrum is similar to those given for freestream conditions by Grande.<sup>6</sup> There is a spike at about 25 kHz that was due to strain gaging<sup>9</sup> of the wire. The contribution of this extraneous signal to the total rms signal was less than about 1% in the freestream and is completely negligible within the boundary layer. The increase in fluctuation level in the freestream beyond about 100 kHz is a broadband, probably facility-generated signal, as verified by using a 5 kHz filter bandwidth. Within the boundary layer, significant amounts of the turbulence energy are contained between about 5 and

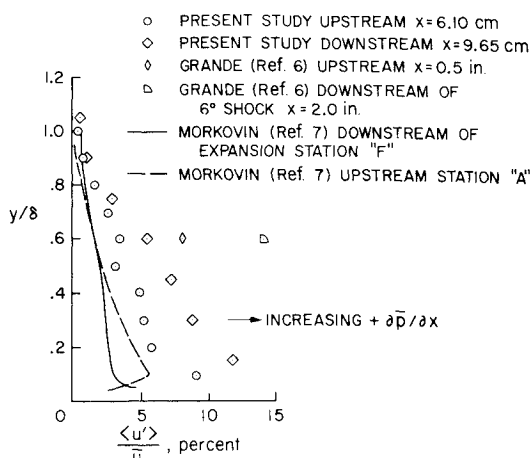


Fig. 8 Effect of pressure gradient on velocity fluctuations.

30 kHz and about 80 to 200 kHz. These frequencies correspond to disturbances whose streamwise length are from about  $10\delta$  to  $\delta$  and about  $\delta/2$  to  $\delta/5$ , respectively.

The spectra within the boundary layer above about 50 kHz do not follow the expected falling trend observed between about 20 and 50 kHz. The flat portions of the spectra above about 50 kHz have not been observed previously. From data obtained in the present study, it is not clear whether these portions of the spectra are solely the result of boundary-layer turbulence or possibly the influence of the freestream turbulence previously discussed.

Since reported values of the turbulence fluctuation data such as  $\langle \rho u' \rangle$  could be affected by these signals above 50 kHz, the influence of possible spurious turbulence energy on the rms values was estimated by the following technique. It was assumed that the lowest energy the spectral curves could have within the boundary layer above 50 kHz would be represented by curves with a falloff slope equal to that observed between about 20 and 50 kHz. The energy contained within these assumed curves and the observed curves of Fig. 6 were obtained and found to be less than about 7% of the total energy for each curve. Thus, if all this energy were spurious, the rms values of the turbulence data would not be more than about 7% too high.

The effect of the pressure gradient on the spectra is shown in Fig. 6 by the data at two downstream stations for a  $y/\delta = 0.5$ . There is predominant increase of turbulence energy in the same range of flow disturbances as previously discussed, i.e.,  $10\delta$  to  $\delta$  and  $\delta/2$  to  $\delta/5$ . Other frequencies exhibit lesser increases.

Oscilloscope traces were obtained at locations of  $y/\delta = 0.1, 0.5$ , and  $0.9$  for the three streamwise stations  $x = 6.10, 9.14$ , and  $11.68$  cm. These traces indicated some qualitative features of the turbulence. In the upstream ( $x = 6.10$  cm) flow at  $y/\delta = 0.9$ , the signal was one-sided indicating boundary-layer intermittency.<sup>1</sup> At  $y/\delta = 0.5$  the signal appeared to be symmetric while at  $y/\delta = 0.1$  a strongly one-sided signal appeared again; however, the sense of the one-sidedness had reversal from that at  $y/\delta = 0.9$ . This phenomenon has also been noted by Kemp and Owen.<sup>3</sup> The downstream traces indicated that the boundary-layer intermittency was preserved and that the one-sided behavior near the wall was greatly increased as a result of the adverse pressure gradient. This latter feature suggests that the momentum transfer near the wall would be increased by the pressure gradient.

### Comparison with Previous Data

The data obtained in the present study are compared with other data for which adiabatic wall conditions prevailed. These comparisons are shown in Figs. 7 and 8.

Figure 7a shows comparisons of data for mass-flux and total-temperature fluctuations. The data presented are for various

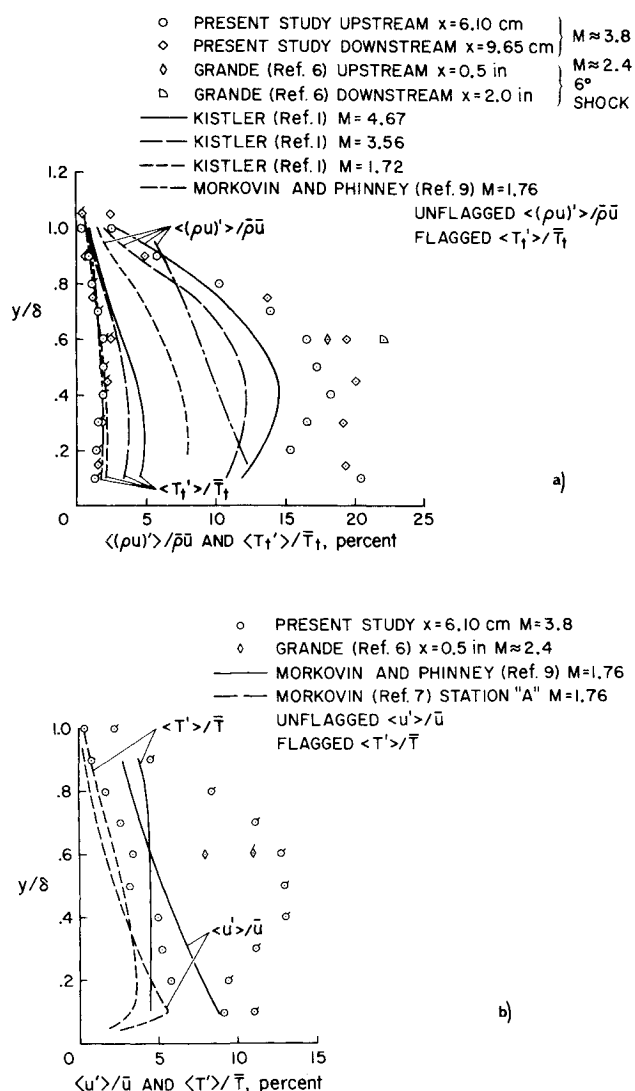


Fig. 7 Comparison of present data with previous data. a) Mass flux and total temperature fluctuations. b) Velocity and static temperature fluctuations.

Mach and Reynolds numbers and for various configurations. Kistler's<sup>1</sup> and Morkovin and Phinney's<sup>9</sup> data are for near-equilibrium flows at Reynolds numbers based on  $\delta$ ,  $Re_\delta$ , of about 5 to 10 times those of the present study. Grande's<sup>6</sup> upstream data like those of the present study were obtained near a nozzle and are not equilibrium flow data. The data most comparable to those of the present study are Kistler's  $M = 3.56$  data. His total temperature fluctuations are about twice those of the present study while the mass flux fluctuations are only about  $\frac{2}{3}$  those of the present study. Grande's mass flux data (he did not report  $\langle T_t' \rangle / \bar{T}_t$ ) agree quite well with the present data. Morkovin and Phinney's data for  $M = 1.76$  are to be compared with Kistler's  $M = 1.72$  data; the total temperature fluctuations agree, but Kistler's  $\langle (\rho u)' \rangle / \bar{\rho} \bar{u}$  data are lower than those of Morkovin and Phinney's data by about 30%. These discrepancies are not clearly understood at present but might be due to the previously cited fact that Kistler's data were obtained in a near equilibrium flow while those of the present study, Grande and Morkovin and Phinney, were not.

Figure 7b shows a comparison of rms velocity and static temperature fluctuations. The velocity fluctuations from the present study are in reasonable agreement with the low Mach number data reported by Morkovin<sup>7</sup> and Morkovin and Phinney.<sup>9</sup> Kovasznay's<sup>8</sup> data is similar to Morkovin's<sup>7</sup> station A data. Grande's velocity fluctuation data appear high. The static temperature fluctuations from the present study agree with Grande's value but are much higher than the low Mach number data.

Figure 8 shows the effect of pressure gradient on velocity fluctuations as evidenced from two quite different flows. Morkovin's flow was a rapid expansion (favorable pressure gradient). Grande's flow and that of the present study are strong adverse pressure gradients. It is clear from Fig. 8 that adverse pressure gradients cause an increase in velocity fluctuations and are a destabilizing influence on the turbulence. This is consistent with our experience with incompressible turbulent flows.

## Conclusions

The specific conclusions that can be derived from the results of this investigation of the turbulence in a shock-wave boundary-layer interaction are as follows.

1) The intensity of the boundary-layer turbulence is increased as a result of the interaction.

2) The fluctuations  $(\rho u)'$  and  $T_t'$  remain highly correlated over most of the boundary layer throughout the interaction.

3) The intensity of the turbulence is increased at certain frequencies more than others at the same  $y/\delta$  as a result of the interaction.

4) The oscilloscope traces show the typical one-sided behavior indicative of intermittency near the boundary-layer edge. This one-sided behavior is reversed near the wall while in the center of the boundary layer the signal is symmetric. The one-sided behavior near the wall is quite predominant just downstream of the interaction.

## References

- Kistler, A. L., "Fluctuation Measurements in a Supersonic Turbulent Boundary Layer," *Physics of Fluids*, Vol. 2, No. 3, May-June 1959, pp. 290-296.
- Wallace, J. E., "Hypersonic Turbulent Boundary-Layer Measurements Using an Electron Beam," NASA SP-216, Dec. 1968.
- Kemp, W. H. and Owen, F. K., "Experimental Study of Nozzle Wall Boundary Layers at Mach Numbers 20 to 47," TN D-6965, Oct. 1972, NASA.
- Fischer, M. C., Maddelon, D. V., Weinstein, L. M., and Wagner, R. D., "Boundary-Layer Pitot and Hot-Wire Surveys at  $M_\infty = 20$ ," *AIAA Journal*, Vol. 9, No. 5, May 1971, pp. 826-834.
- Laderman, A. J. and Demetriades, A., "Measurements of the Mean and Turbulent Flow in a Cooled-Wall Boundary Layer at Mach 9.37," AIAA Paper 72-73, San Diego, Calif., 1972.
- Grande, E., "An Investigation of the Unsteady Flow Properties of the Interaction Between a Shock Wave Turbulent Boundary Layer in Two-Dimensional Internal Flow," Ph.D. thesis, 1971, Univ. of Washington, Seattle, Wash.
- Morkovin, M. V., "Effects of High Acceleration on a Turbulent Supersonic Shear Layer," *Proceedings of the 1955 Heat Transfer and Fluid Mechanics Institute*, Stanford Univ. Press, Stanford, Calif., 1955.
- Kovasznay, L. S. G., "Turbulence in Supersonic Flow," *Journal of Aeronautical Science*, Vol. 20, No. 10, Oct. 1953, p. 657.
- Morkovin, M. V., "Extended Applications of Hot-Wire Anemometry to High-Speed Turbulent Boundary Layers," AFOSR TN-58-469, ASTIA AD-158-279, June 1958, Dept. of Aeronautics, Johns Hopkins University, Baltimore, Md.
- Rose, W. C., "The Behavior of a Compressible Turbulent Boundary Layer in a Shock-Wave Induced Adverse Pressure Gradient," Ph.D. thesis, 1972, Univ. of Washington, Seattle, Wash.; also available as TN D-7092, March 1973, NASA.
- Kovasznay, L. S. G., "The Hot Wire Anemometer in Supersonic Flow," *Journal of Aeronautical Sciences*, Vol. 17, 1950, pp. 565-572.